The Influence of the Amino Acid Transporter LAT1 on Patient Prognosis and the Relationships between Tumor Immunometabolic and Proliferative Features Depend on Menopausal Status in Breast Cancer

Gautham Ramshankar[1,2], Ryan Liu[2,3], and Rachel J. Perry[2]*

[1]Irvington High School, Fremont, CA
[2]Departments of Cellular & Molecular Physiology and Internal Medicine (Endocrinology), Yale School of Medicine, New Haven, CT
[3]Cedar Park High School, Cedar Park, TX
*Correspondence to: rachel.perry@yale.edu

Abstract

L-type Amino Acid Transporter 1 (LAT1) facilitates the uptake of specific essential amino acids, and due to this quality, it has been correlated to worse patient outcomes in various cancer types. However, the relationship between LAT1 and various clinical factors, including menopausal status, in mediating LAT1's prognostic effects remains incompletely understood. This is particularly true in the unique subset of tumors that are both obesity-associated and responsive to immunotherapy, including breast cancer. To close this gap, we employed 6 sets of transcriptomic data using the Kaplan-Meier model in the Xena Functional Genomics Explorer, demonstrating that higher LAT1 expression diminishes breast cancer patients' survival probability. Additionally, we analyzed 3′-Deoxy-3′-^{18}F-Fluorothymidine positron emission tomography-computed tomography (^{18}F-FLT PET-CT) images found on The Cancer Imaging Archive (TCIA). After separating all patients based on menopausal status, we correlated the measured ^{18}F-FLT uptake with various clinical parameters quantifying body composition, tumor proliferation, and immune cell infiltration. By analyzing a wealth of deidentified, open-access data, the current study investigates the impact of LAT1 expression on breast cancer prognosis, along with the menopausal status-dependent associations between tumor proliferation, immunometabolism, and systemic metabolism.

Introduction

As the second leading cause of cancer deaths in women, breast cancer has become a major clinical and social burden, with annual out-of-pocket costs for breast cancer care in the U.S. exceeding $3 billion in 2019 [1]. Because breast cancer has high economic and social costs, it has become increasingly necessary to identify potential risk factors, biomarkers, and treatments. Nearly 30% of breast cancer deaths are caused by modifiable risk factors like excess body

weight and alcohol consumption [2]. Several of the modifiable risk factors that predispose to breast cancer converge on metabolism. Consequently, a key priority in the cancer field has been to investigate tumor metabolism and how it can be affected by a patient's lifestyle. In the 1920s, Otto Warburg discovered that in order to sustain their energetic needs while prioritizing generating the biomass and nucleotides required for rapid proliferation and growth, cancer cells have greater metabolic demands than their benign counterparts. Because of this, oncogenic metabolism is characterized by heightened glycolytic metabolism, which necessitates greater uptake of glucose. This phenomenon is now called the Warburg Effect and has greatly shaped the field of tumor metabolism [3]. However, many years after Warburg's groundbreaking work identifying glucose metabolism as a key contributor to tumor pathogenesis, there remains relatively less investigation into the role of amino acid metabolism in tumor progression. The same can be said about amino acid metabolic reprogramming, the abnormal changes to amino acid uptake or metabolic pathways caused by tumor progression. However, past literature has shown that low concentrations of amino acids in the tumor microenvironment inhibit nearby immune cells, weakening immune responses to tumor cells and contributing to tumor progression [4,5]. These data beg further investigation of the tumor- and/or immune cell-centric metabolic role of amino acids in the tumor microenvironment.

In order to leave the tumor interstitial compartment and undergo metabolism by tumor cells, amino acids must cross the plasma membrane with the help of amino acid transporters. Amino acid transporters can thus facilitate the uptake of amino acids to meet the metabolic needs of cancer cells, explaining why the expression of these transporters has been associated with the proliferation of cancer cells. One such transporter, L-type amino acid transporter 1 (LAT1) is particularly important in the amino acid transport process [4]. Encoded by the gene Solute Carrier Family 7 Member 5 (*SLC7A5*), LAT1 is a light-chain protein that heterodimerizes with its heavy-chain partner 4F2hc (*SLC3A2*) through a conserved disulfide bridge, forming the human LAT1-4F2hc complex. A sodium-independent transporter, LAT1 is an integral membrane protein that mediates the transport of large neutral amino acids like methionine, leucine, and histidine by exchanging them with intracellular glutamine [6]. LAT1 is unique in that it transports multiple essential amino acids, which cannot be synthesized by the human body and must be obtained through diet [7,8]. Considering the dietary dependence of its transported molecules, LAT1 is a particularly intriguing target to participate in the links between lifestyle, systemic metabolism, and cancer.

Positron emission tomography-computed tomography (PET-CT) is a powerful tool in cancer metabolism research due to its ability to visualize thin slices of tissue in vivo and quantify cells' metabolic activity by measuring radiotracers like 3′-Deoxy-3′-^{18}F-Fluorothymidine (^{18}F-FLT). An analog of the nucleoside thymidine, ^{18}F-FLT is phosphorylated by the cytosolic enzyme thymidine kinase 1 (TK1) and taken up into the cell. During the S-phase of the cell cycle, TK1 is overexpressed nearly tenfold and ^{18}F-FLT uptake is at its highest. In this way, concentrations of

^{18}F-FLT and TK1 are elevated in cancer cells, making ^{18}F-FLT uptake a quantitative marker for tumor proliferation [9–12]. Ki-67 is a nuclear nonhistone protein, and because it is only expressed in cells that are not in the G_0 phase of the cell cycle, it can only be observed in actively-proliferating cells. This quality has made Ki-67 a classic proliferative marker for tumor cells [13], and is included in the datasets analyzed in the current report.

Past studies have demonstrated that menopausal status affects to what extent obesity is a risk factor for developing breast cancer. In multiple studies, obesity has been observed to have a protective relationship with breast cancer risk in premenopausal patients whereas it is a risk factor for breast cancer in postmenopausal patients [14]. Because of this, we segmented our analyses based on patients' menopausal statuses. We used body mass index (BMI) in kg/m^2 as a metric for obesity. By analyzing PET-CT scans of 58 patients from The National Cancer Imaging Archive (TCIA), we correlate patients' calculated ^{18}F-FLT uptake and Ki-67 index values to their BMIs to study the relationship between obesity and breast cancer [10,15,16].

To demonstrate the relationship between LAT1 and poorer health outcomes with a larger sample size, we leveraged RNA-seq data in the UCSC Xena Functional Genomics Explorer [17]. This allowed us to visualize the effect of LAT1 expression on breast cancer prognosis in premenopausal and postmenopausal patients. Ultimately, we used a similar workflow to our prior published work to examine the impact of SLC7A5, a gene with a drastically different role in metabolism, in breast cancer [18]. Our analyses reveal new insights into the associations between clinical variables (obesity, menopausal status), cell proliferation, infiltration with multiple immune cell subtypes, tumor LAT1 expression, and survival in breast cancer patients, which deepen our understanding of the bidirectional relationships that may inform interventional studies targeting these variables in individuals with breast cancer.

Methods

^{18}F-FLT PET-CT Quantitative Image Analysis

Deidentified PET-CT images produced during the ACRIN 6688 clinical trial [10] were obtained from The Cancer Imaging Archive (TCIA). This dataset, "ACRIN-FLT-Breast (ACRIN 6688)", can be found here: https://wiki.cancerimagingarchive.net/pages/viewpage.action?pageId=30671268. Because only publicly available, deidentified data were analyzed, separate ethical approval is not required. We analyzed the scans of all patients with a menopausal status, height, weight, and 5 clear CT slices (i.e., slices in which the primary breast tumor could be identified and its corresponding SUV values could be generated) present in the dataset. 58 of the 90 enrolled patients in the ACRIN clinical trial met these criteria, and all were analyzed. Of these 58 patients, 26 were premenopausal and 32 were postmenopausal. Scans taken at 3 different dates were available for most patients, and we used the earliest scan (from the baseline scanning which was defined to be 4 weeks before any treatment was administered) to minimize the chemotherapeutic effect of the

treatment used in the clinical trial. Likewise, heights and weights measured on patients' first visits were used. These data were selected for analysis because breast cancer treatment often causes some weight gain [19–22], which may obscure differences in BMI that could promote proliferation.

The patients' images were uploaded to Fiji ImageJ and we used the PET-CT Viewer plugin to view and analyze them. After identifying the primary breast tumor on the PET image, we selected the tumor and used the Brown Fat Volume tool to draw fixed-volume spheres around the interior regions of interest (ROIs) on the CT slice. 5 slices were used from each patient's scan. SUV parameters were set at 2 to 15, and ^{18}F-FLT uptake was calculated in the tumor tissue in the specified ROI. ^{18}F-FLT uptake on PET-CT scans is measured by calculating and recording lean body mass-corrected standardized uptake values (SUV) of which there are 3 types: SUV_{Mean}, SUV_{Max}, and SUV_{Peak}. After positioning a fixed-volume sphere on a tumor, within the ROI, SUV_{Mean} represents the average SUV, SUV_{Max} indicates the maximum SUV, and SUV_{Peak} corresponds to the SUV derived from a localized cluster of voxels with high uptake [10,23]. The primary endpoint of image analysis was BMI (kg/m^2) correlated to the 3 types of tumor SUV (g/mL).

LAT1 Prognostic Analysis

Using the UCSC Xena Functional Genomics Browser (https://xenabrowser.net/), we accessed the "TCGA Breast Cancer (BRCA) cohort" (found here: https://xenabrowser.net/datapages/?cohort=TCGA%20Breast%20Cancer%20(BRCA)&removeHub=http%3A%2F%2F127.0.0.1%3A7222) which included 2 datasets. The BRCA cohort had 1247 total patients, and all of them had menopausal statuses recorded, which we accessed through the "Phenotypes" dataset: https://xenabrowser.net/datapages/?dataset=TCGA.BRCA.sampleMap%2FBRCA_clinicalMatrix&host=https%3A%2F%2Ftcga.xenahubs.net&removeHub=https%3A%2F%2Fxena.treehouse.gi.ucsc.edu%3A443. 1236 of the 1247 patients had survival data recorded. The "IlluminaHiSeq" dataset was used to study LAT1 expression and it can be found here: https://xenabrowser.net/datapages/?dataset=TCGA.BRCA.sampleMap%2FHiSeqV2&host=https%3A%2F%2Ftcga.xenahubs.net&removeHub=http%3A%2F%2F127.0.0.1%3A7222. The "IlluminaHiSeq" dataset used fragments per kilobase of exon per million mapped fragments (FPKM) to measure gene expression. Again, only openly available human data were analyzed. 1218 of the 1247 patients had LAT1 expression data. These datasets were used alongside the Kaplan-Meier model in the Xena visualization suite to analyze LAT1 and its effect on breast cancer prognosis.

To analyze LAT1 expression, the following workflow was used: the 1247 patients were added to Column A. SLC7A5 was added to Column B as a genomic variable with the gene expression dataset selected, and menopause status was added to Column C as a phenotypic variable. After

removing null and duplicate samples, a Kaplan-Meier (KM) plot was generated in Column B to show LAT1 expression and its effect on prognosis in 1005 of the 1247 patients. Next, low and high-expression groups were created from these patients. After 34 patients with indeterminate menopausal statuses were removed from the dataset, 10.46 FPKM was calculated by Xena to be the median for LAT1 expression. Patients were divided at the median: 485 patients were in the low expression group (< 10.46 FPKM), and 486 patients were in the high expression group (>= 10.46 FPKM). A KM plot was generated for each group using Column C, creating 2 KM plots with the premenopausal, perimenopausal, and postmenopausal patients in each expression group.

In addition to the BRCA dataset, the following datasets were used to access breast cancer patients' gene expression data: "RSEM norm-count" from the "TCGA TARGET GTEx" cohort (https://xenabrowser.net/datapages/?dataset=TcgaTargetGtex_RSEM_Hugo_norm_count&host=https%3A%2F%2Ftoil.xenahubs.net&removeHub=https%3A%2F%2Fxena.treehouse.gi.ucsc.edu%3A443), "Desmedt 76 Gene Node-Neg Gene Exp" from the "node-negative breast cancer (Desmedt 2007)" cohort (https://xenabrowser.net/datapages/?dataset=desmedt2007_public%2Fdesmedt2007_genomicMatrix&host=https%3A%2F%2Fucscpublic.xenahubs.net&removeHub=https%3A%2F%2Fxena.treehouse.gi.ucsc.edu%3A443), "gene expression RNAseq - US projects" from the "ICGC (donor centric)" cohort (https://xenabrowser.net/datapages/?dataset=donor%2Fexp_seq.all_projects.donor.USonly.xena.tsv&host=https%3A%2F%2Ficgc.xenahubs.net&removeHub=https%3A%2F%2Fxena.treehouse.gi.ucsc.edu%3A443), "Gene Expression" from the "Breast Cancer (Chin 2006)" cohort (https://xenabrowser.net/datapages/?dataset=chin2006_public%2Fchin2006Exp_genomicMatrix&host=https%3A%2F%2Fucscpublic.xenahubs.net&removeHub=https%3A%2F%2Fxena.treehouse.gi.ucsc.edu%3A443), and "Miller TP53 Gene Exp" from the "Breast Cancer (Miller 2005)" cohort (https://xenabrowser.net/datapages/?dataset=miller2005_public%2Fmiller2005_genomicMatrix&host=https%3A%2F%2Fucscpublic.xenahubs.net&removeHub=https%3A%2F%2Fxena.treehouse.gi.ucsc.edu%3A443). To measure expression, the "TCGA TARGET GTEx" dataset used FPKM, the "ICGC (donor centric)" dataset used normalized read count, and the "Node-negative breast cancer (Desmedt 2007)" and "Breast Cancer (Miller 2005)" datasets used log2 units. Although these gene expression datasets did not include menopausal status as a possible phenotypic variable, our selection criteria were to include breast cancer datasets that had RNA-seq data on SLC7A5 and survival data from the same patients that could be used to produce Kaplan-Meier plots on the Xena platform. Each dataset was used in the same way: SLC7A5 was selected as a genomic variable in Column B, and after null and duplicate samples were removed, a KM plot was generated. For the "TCGA TARGET GTEx" and "ICGC (donor centric)" datasets, only patients with breast tumors were selected for the analysis.

All of the KM plots were created with Overall Survival as the dependent variable unless otherwise specified. After patients were split at the median for the gene expression analyses, some groups had an unequal number of patients because patients with the same expression levels were put in the same group. Some patients were at the expression median, and the median was calculated to ensure they were placed in the high-expression group while keeping the sizes of each expression group roughly the same.

Statistical Analysis

Correlation tests were performed between patients' SUV and BMI values. 26 premenopausal patients' BMIs ranged from 23.829 to 142.822 kg/m^2 (mean [SD] = 33.972 [22.584]), and 32 postmenopausal patients' BMIs ranged from 17.940 to 199.219 kg/m^2 (mean [SD] = 40.865 [36.818]). The unusually high BMI values are driven by unusually low heights reported for these patients; however, only one premenopausal and postmenopausal patient had a reported BMI above 100. Because 5 slices were used per patient, each patient had 5 SUV_{Max} values and 5 SUV_{Peak} values but only 1 BMI. In order to correlate BMI and SUV, we needed the same number of values for each. In order to get one SUV for each patient, we took the mean of the SUVs produced from all 5 slices. For SUV_{Mean}, the calculated SUV had a margin of error indicated by a plus-minus sign. This meant that the calculation of each SUV_{Mean} yielded 2 numerical values, one being the high value and the other being the low value, so 5 slices yield 10 SUV_{Mean} values per patient. We took the mean of these 10 values for each patient. Each of these individual SUVs was then correlated with each patient's BMI.

We also correlated each patient's 3 types of SUVs to their Ki-67 values to further inform the validity of ^{18}F-FLT uptake as a metric for tumor proliferation. BMI was also correlated to Ki-67. All correlations were two-tailed Pearson correlation tests performed after patients' data were segmented by menopausal status. Shapiro-Wilk tests were also performed to determine if any groups of data were normally distributed. Student's t-tests and Mann-Whitney U tests were performed on parametric and nonparametric data, respectively, to assess difference. For both tests, all data were transformed using log2 fold changes of the mean.

Unless otherwise specified, statistical analysis was done and graphs were made in Python 3.9 using the pandas (version 1.5) and SciPy (version 1.10) libraries. The two-tailed Pearson correlation tests were conducted using the "pearsonr" function from the scipy.stats module. The Mann-Whitney U tests were conducted using the "mannwhitney" function, the Student's t-tests were conducted using the "ttest_ind" function, and the Shapiro-Wilk tests were performed using the "shapiro" function, all from the scipy.stats module. All Python code can be found here: https://github.com/gramshankar/LAT1BreastCancer. For each of the KM plots, a log-rank test was conducted by Xena to compare the curves in the graph. Test statistics and p-values were calculated. Statistical significance was indicated by p-values less than 0.05, and marginally

significant results have p-values greater than 0.05 but less than 0.10.

Results

Correlation analysis between proliferative markers, obesity, and immune cells by menopausal status

In premenopausal patients, Ki-67 insignificantly positively correlated with SUV_{Mean}, SUV_{Peak} (marginal significance), and SUV_{Max} (marginal significance) (Fig 1A). However, the relationship between Ki-67 and tumor ^{18}F-FLT uptake was statistically stronger in postmenopausal patients, in whom Ki-67 significantly positively correlated with SUV_{Mean}, SUV_{Peak}, and SUV_{Max} (Fig 1B).

In premenopausal patients, BMI insignificantly negatively correlated with SUV_{Mean}, SUV_{Peak}, and SUV_{Max} (Fig 1A). In postmenopausal patients, BMI insignificantly positively correlated with SUV_{Mean} (marginal significance), SUV_{Peak}, and SUV_{Max} (Fig 1B). In premenopausal and postmenopausal patients, BMI insignificantly positively correlated with Ki-67 (Fig 1A, Fig 1B).

In premenopausal patients, basophil, eosinophil, neutrophil, monocyte, and lymphocyte counts insignificantly negatively correlated with SUV_{Mean}, SUV_{Peak}, and SUV_{Max}. White blood cell counts insignificantly positively correlated with SUV_{Mean}, SUV_{Peak}, and SUV_{Max}. All immune cells insignificantly negatively correlated with Ki-67 (Fig 1A).

In postmenopausal patients, basophil, eosinophil, monocyte, white blood cell, and lymphocyte counts insignificantly positively correlated with SUV_{Mean}, SUV_{Peak}, and SUV_{Max}. Neutrophil counts insignificantly negatively correlated with SUV_{Mean}, SUV_{Peak}, and SUV_{Max}. Basophil, eosinophil, monocyte, and lymphocyte counts insignificantly negatively correlated with Ki-67. Neutrophil and white blood cell counts insignificantly positively correlated with Ki-67 (Fig 1B).

In premenopausal patients, BMI negatively correlated with basophil, eosinophil, monocyte, and lymphocyte counts and positively correlated with neutrophil and white blood cell counts (Fig 1A). Opposite relationships were observed in postmenopausal patients, in whom BMI positively correlated with basophil, eosinophil, monocyte, and lymphocyte counts and negatively correlated with neutrophil and white blood cell counts (Fig 1B).

These correlation tests' p-values are presented in Tables 1 - 4. In addition, the results from the Mann-Whitney and Student's t-tests performed are presented in Tables 5 - 8.

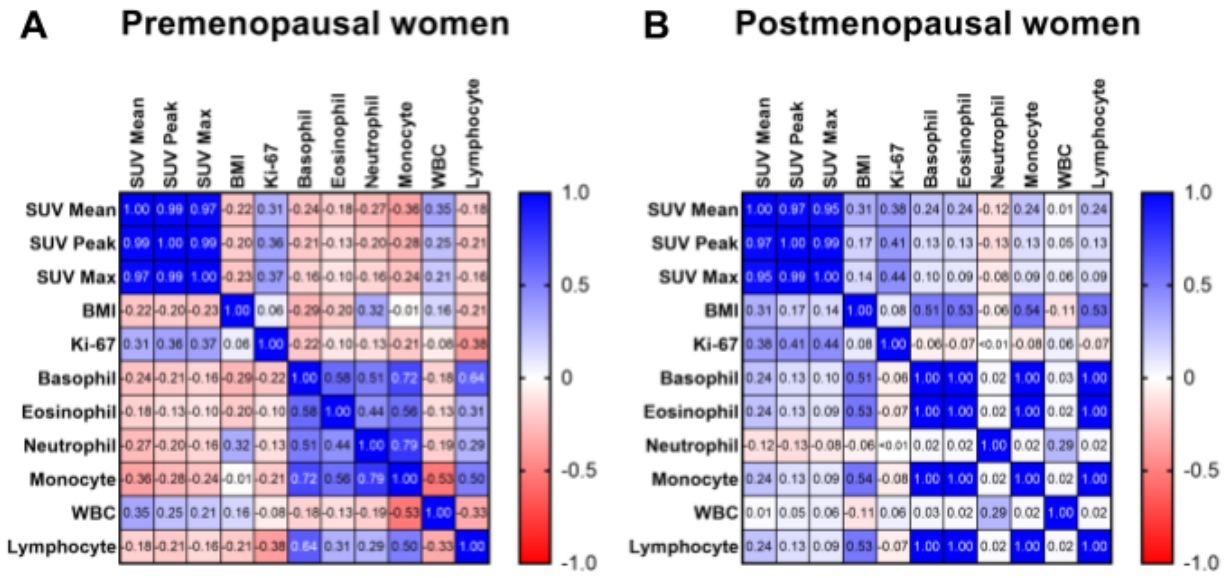

Fig 1. Correlations between clinical variables. Proliferative markers (Ki-67 and lean body mass-corrected ^{18}F-FLT uptake measured by SUV_{Mean}, SUV_{Peak}, and SUV_{Max}), obesity (BMI), and immune cell counts (basophil, eosinophil, neutrophil, monocyte, white blood cell, and lymphocyte) were correlated in **(A)** premenopausal and **(B)** postmenopausal patients. Pearson r values were calculated and correlation matrices were generated in GraphPad Prism version 9.5.1.

	Premenopausal Patients	Postmenopausal Patients
SUV_{Mean}	0.114	**0.035**
SUV_{Peak}	***0.081***	**0.045**
SUV_{Max}	***0.078***	**0.029**

Table 1. P-values from correlations between Ki-67 and ^{18}F-FLT uptake. Significant results are bolded and marginally significant results are bolded and italicized.

	Premenopausal Patients	Postmenopausal Patients
SUV_{Mean}	0.279	***0.095***
SUV_{Peak}	0.335	0.342
SUV_{Max}	0.268	0.437
Ki-67	0.767	0.691

Table 2. P-values from correlations between BMI and proliferative markers. Marginally significant results are bolded and italicized.

281

	Basophils	Eosinophils	Neutrophils	Monocytes	WBC	Lymphocyte
SUV_{Mean}	0.395	0.539	0.334	0.190	0.170	0.472
SUV_{Peak}	0.401	0.620	0.420	0.262	0.326	0.404
SUV_{Max}	0.519	0.691	0.520	0.342	0.408	0.537
Ki-67	0.394	0.712	0.626	0.417	0.769	0.132

Table 3. P-values from correlations between immune cells and proliferative markers in premenopausal patients.

282

	Basophils	Eosinophils	Neutrophils	Monocytes	WBC	Lymphocyte
SUV_{Mean}	0.239	0.237	0.671	0.235	0.927	0.233
SUV_{Peak}	0.560	0.563	0.586	0.560	0.913	0.561
SUV_{Max}	0.682	0.685	0.741	0.679	0.946	0.681
Ki-67	0.781	0.737	0.986	0.723	0.783	0.762

Table 4. P-values from correlations between immune cells and proliferative markers in postmenopausal patients.

283

	Premenopausal Patients	Postmenopausal Patients
SUV_{Mean}	0.959	0.291
SUV_{Peak}	0.926	0.528
SUV_{Max}	0.992	0.436

Table 5. Mann-Whitney U tests identify no significant differences between the log2 fold change in Ki-67 and ^{18}F-FLT uptake in pre- or postmenopausal patients. P-values are shown.

284

	Premenopausal Patients		Postmenopausal Patients	
	Test Statistic	P-value	Test Statistic	P-value
SUV_{Mean}	357	0.735	722	**0.004**
SUV_{Peak}	277	0.268	618	0.157
SUV_{Max}	295	0.437	614	0.173
Ki-67	226	0.205	393	0.993

Table 6. Mann-Whitney U tests identify differences between the log2 fold change in BMI and SUV_{Mean} in postmenopausal patients, but no other proliferative markers differed in pre- or postmenopausal patients.

285

	Basophils	Eosinophils	Neutrophils	Monocytes	White Blood Cells	Lymphocytes
SUV_{Mean}	0.339	0.619	0.213	0.184	0.803	0.115
SUV_{Peak}	0.339	0.803	0.319	0.229	0.431	0.147
SUV_{Max}	0.318	0.803	0.431	0.340	0.481	0.171
Ki-67	0.755 [a]	0.901	0.135	0.584 [a]	0.142 [a]	0.245

Table 7. Mann-Whitney U and Student's t-tests identify differences between Immune Cells and Proliferative Markers in Premenopausal Patients. The log2 fold change of each parameter was compared. The comparisons' p-values are shown above. Shapiro-Wilk tests were used to assess the data's normality. Based on these results, normally distributed data were compared using the Student's t-test, and all other analyses used the Mann-Whitney test.
[a] These comparisons use the Student's t-test.

	Basophils	Eosinophils	Neutrophils	Monocytes	White Blood Cells	Lymphocytes
SUV_{Mean}	**<0.001**	**<0.001**	0.235	**<0.001**	0.792	**<0.001**
SUV_{Peak}	**<0.001**	**<0.001**	0.187	**<0.001**	0.345	**<0.001**
SUV_{Max}	**<0.001**	**<0.001**	0.124	**<0.001**	0.244	**<0.001**
Ki-67	**0.010**	**<0.001**	***0.091***	**0.002**	0.379	**<0.001**

Table 8. Mann-Whitney U tests identify differences between immune cells and proliferative markers in postmenopausal patients. The log2 fold change of each parameter was compared. The comparisons' p-values are shown above. Significant results are bolded, and marginally significant results are bolded and italicized.

LAT1 Expression and Survival Probability

In the TCGA BRCA gene expression dataset, patients in the high LAT1 expression group experienced lower overall survival than patients in the low expression group until 4000 days after initial treatment. From that point until 6500 days and again from 6600 days until 7500 days, the low LAT1 expression group had a worse overall survival rate (Fig 2A). Similarly, patients with high LAT1 expression had a lower disease-specific survival rate than patients with low LAT1 expression until 4400 days; after that point until the end of the study, patients in the low expression group had a lower disease-specific survival rate (Fig 2B).

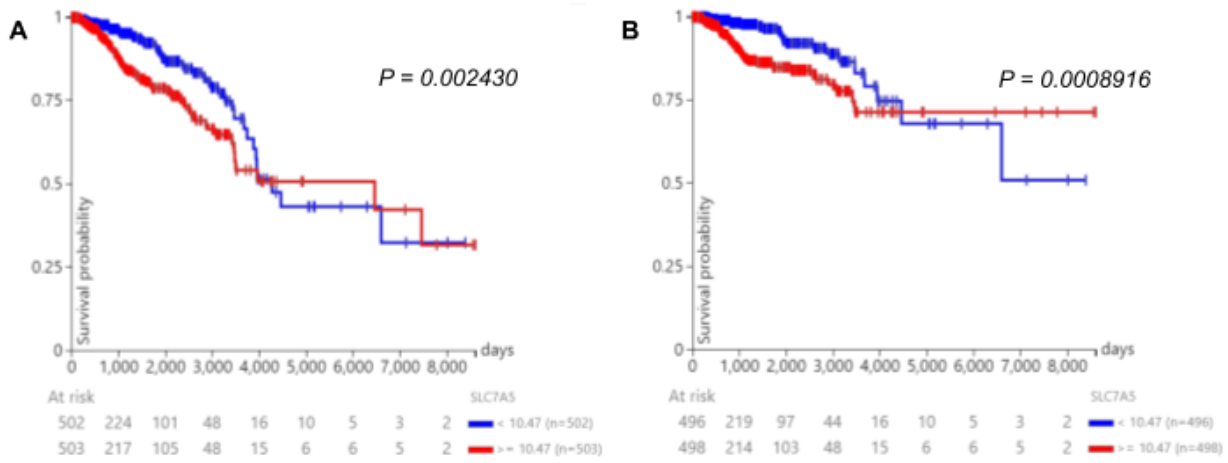

Fig 2. LAT1 expression and prognosis in TCGA BRCA patients. Prognosis in patients from the TCGA BRCA gene expression dataset. Patients were separated into high (>= 10.47 FPKM) and low (< 10.47 FPKM) LAT1 expression groups, and **(A)** overall survival and **(B)** disease-specific survival were observed up to 8605 days after initial treatment. The median for expression level is slightly different from the median stated earlier because patients with indeterminate menopausal status were included in this analysis.

In the "TCGA TARGET GTEx" gene expression dataset, patients in the high LAT1 expression group (>= 10.65 FPKM) experienced lower survival rates than the low LAT1 expression group (< 10.65 FPKM) until 4000 days after initial treatment. From 4000 days until the end of the study, the low-expression group had a lower survival rate (Fig 3A). In the "Node-negative breast cancer (Desmedt 2007)" gene expression dataset, after the first 500 days, the high LAT1 expression group (>= 0.1221 log2) experienced a lower survival rate than the low LAT1 expression group (< 0.1221 log2) for the remainder of the study (Fig 3B). In the "ICGC (donor centric)" gene expression dataset, the high LAT1 expression group (>= 0.00002400) had lower survival than the low LAT1 expression group (< 0.00002400) for the entire study. The high expression group's survival probability reached 0% near 4000 days (Fig 3C). In the "Breast Cancer (Chin 2006)" gene expression dataset, except from 1.2 to 1.4 years, the high LAT1 expression group experienced a lower survival rate than the low LAT1 expression group. Units were not given for this study but it most likely used log2 units (Fig 3D). In the "Breast Cancer (Miller 2005)" gene expression dataset, overall survival data were not available so disease-specific survival was observed. The high LAT1 expression group (>= -0.1707 log2) experienced worse survival than the low LAT1 expression group (< -0.1707 log2) for the entire study (Fig 3E). Overall, 2 of the gene expression datasets showed that low LAT1 expression conferred a poorer prognosis in breast cancer patients than high LAT expression, while 4 others showed the opposite.

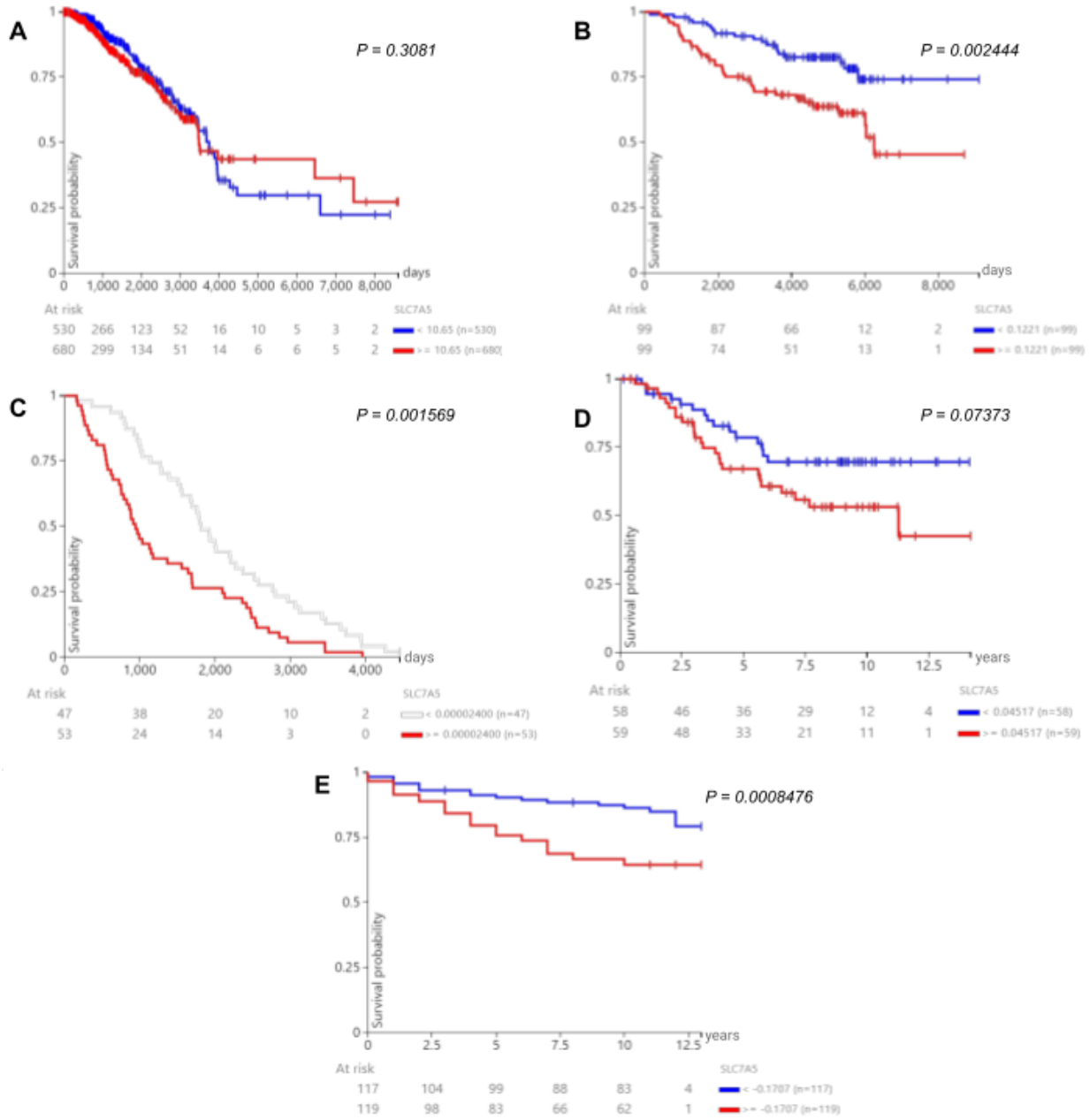

Fig 3. LAT1 expression and prognosis in patients from other datasets. After patients were separated into high and low LAT1 expression groups, survival was observed in patients from the **(A)** "TCGA TARGET GTEx", **(B)** "Node-negative breast cancer (Desmedt 2007)", **(C)** "ICGC (donor centric)", **(D)** "Breast Cancer (Chin 2006)", and **(E)** "Breast Cancer (Miller 2005)" cohorts.

Survival probability with high LAT1 expression TCGA BRCA patients by menopausal status

The impact of menopausal status on survival in patients with high LAT1 expression is shown in Fig 4. After 1000 days, postmenopausal patients had the lowest survival rates. Premenopausal patients had the highest survival rates among the 3 groups until approximately 2500 days, from

which point peri-menopausal patients had the highest survival until 3600 days (Fig 4); however, our ability to draw conclusions regarding survival in peri-menopausal patients is limited by the relatively low number of patients in this group.

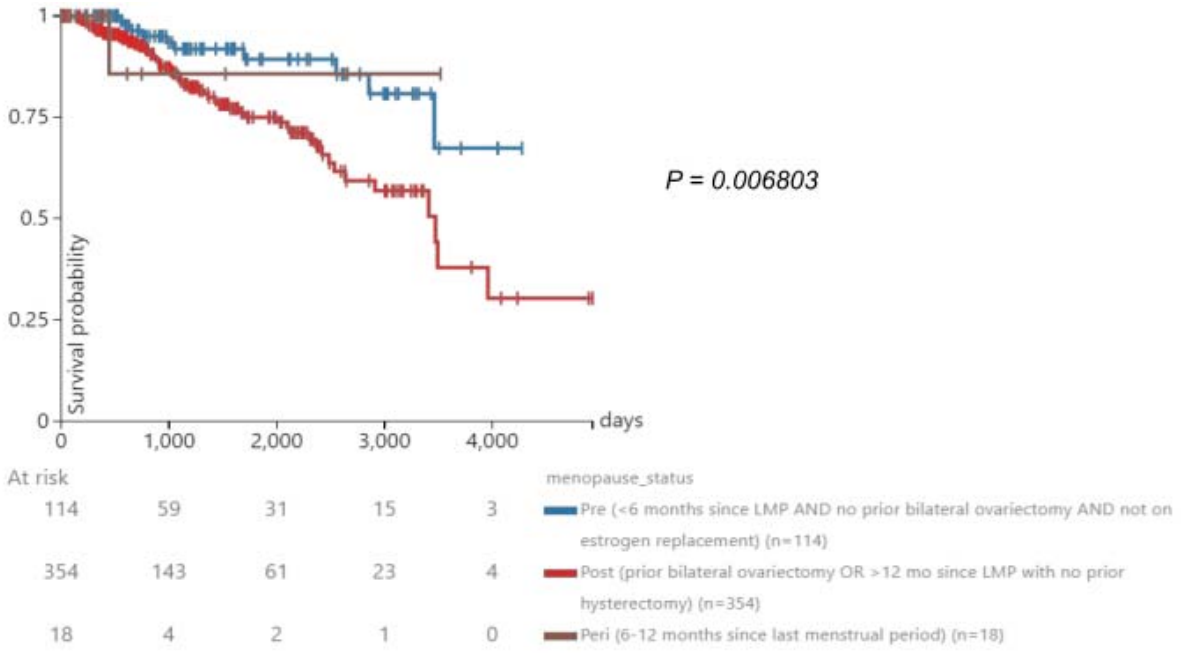

Fig 4. High expression and prognosis in TCGA BRCA patients. Prognosis in the high expression group (>= 10.46 FPKM) from the TCGA BRCA gene expression dataset. The high expression group was separated into 3 groups: premenopausal, postmenopausal, and peri-menopausal breast cancer patients.

Survival probability with low LAT1 expression TCGA BRCA patients by menopausal status

The impact of menopausal status on survival in patients with low LAT1 expression is shown in Fig 5. Premenopausal patients had a higher survival rate than postmenopausal patients until 3200 days. Postmenopausal patients, after 3200 days and until the end of the available survival data for premenopausal patients at approximately 3800 days, exhibited a higher survival rate compared to premenopausal patients. The few peri-menopausal patients in this study maintained a 100% survival probability throughout the duration that they were monitored.

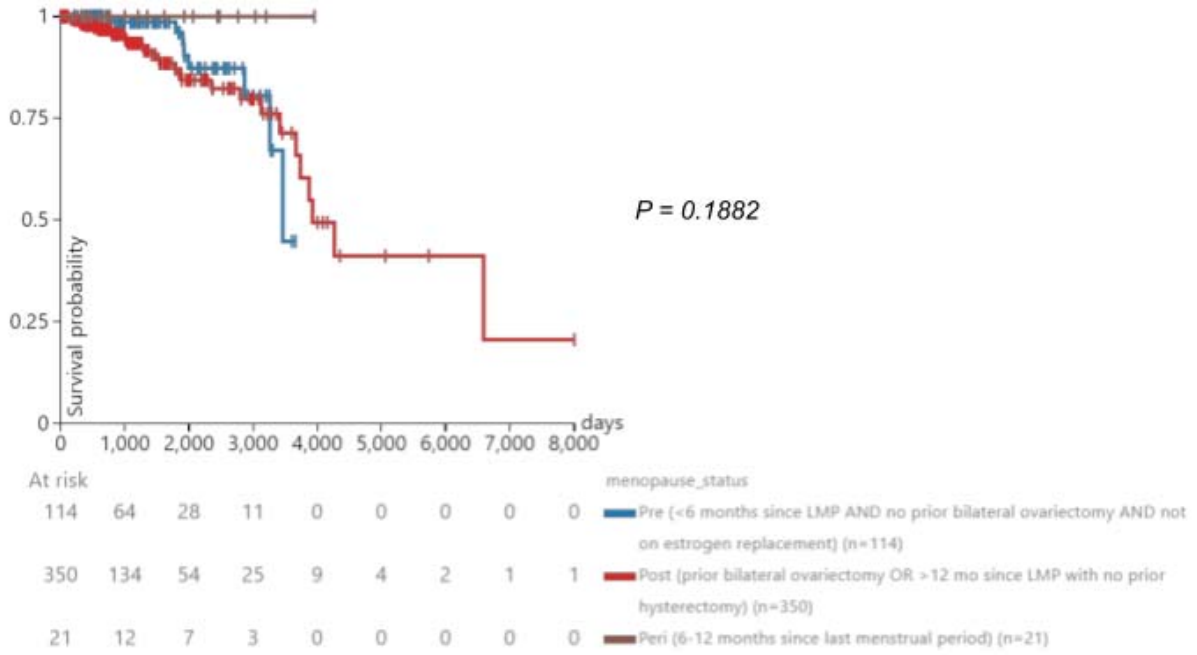

Fig 5. Low expression and prognosis in TCGA BRCA patients. Prognosis in the low expression group (< 10.46 FPKM) from the TCGA BRCA gene expression dataset. The low expression group was separated into 3 groups: premenopausal, postmenopausal, and peri-menopausal breast cancer patients.

Discussion

Increasing interest in the relationship between systemic metabolism, tumor metabolism, immunometabolism, and cancer outcomes, alongside evolving technologies expanding both the available data and the community's ability to mine it to develop new insights. To that end, in this study, we utilized multiple publicly available breast cancer datasets, including "ACRIN-FLT-Breast (ACRIN 6688)", TCGA BRCA "Phenotypes", TCGA BRCA "IlluminaHiSeq", "TCGA TARGET GTEx", "Node-negative breast cancer (Desmedt 2007)", "ICGC (donor centric)", "Breast Cancer (Chin 2006)", and "Breast Cancer (Miller 2005)", aiming to better understand the intersection between parameters of systemic metabolic health, tumor gene expression, and immune cell infiltration, and outcomes in individuals with breast cancer (Fig 6).

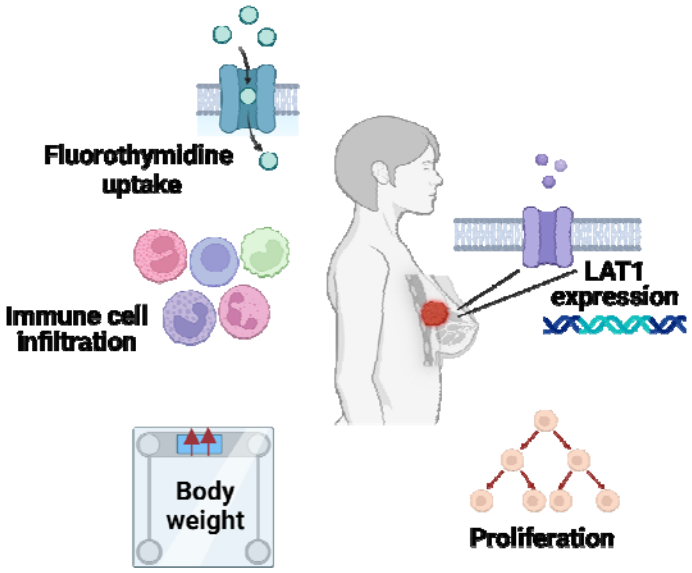

Fig 6. Summary of factors correlated in this analysis. Figure created with BioRender.com.

As opposed to genes or metabolic fluxes involved in glucose [24–31]or lipid metabolism [31–39], there exists a relative paucity of studies exploring the impact of expression of genes regulating amino acid uptake in breast cancer. Therefore, we elected to focus the current study on the expression of LAT1, which transports large amino acids including leucine, isoleucine, valine, phenylalanine, methionine, tyrosine, histidine, and tryptophan into the cell, and its relationships with body weight, tumor cell proliferation, and immune infiltration. Prior literature indicates that LAT1 is involved in protein synthesis [40,41] and mTORC1 activity [42,43], and may also modulate the anti-tumor immune response [44–47]. Overexpression of LAT1 has been observed in a plethora of tumor types ranging from lung to endometrial to liver, but fewer studies of the relationship between LAT1 and breast cancer exist [48]. Furthermore, LAT1 has been less frequently associated with a poor long-term clinical prognosis in breast cancer than in other cancers. Our data, too, provide mixed evidence: while some datasets showed that high LAT1 expression was worse for prognosis, others showed the opposite. Namely, the BRCA dataset showed that low LAT1 expression conferred worse survival at some points. This is likely because when compared to the high-expression group, a greater proportion of low-expression patients in the BRCA dataset had a positive margin status. Also, a greater percentage of the low-expression group had a distant metastasis present. The fact that the low LAT1 expression group tended to have more positive margin status and distant metastases than patients in the high-expression group may contribute to the discrepancy between our data on the predictive value of LAT1 versus others, as these have shown to be poor prognostic factors in breast cancer [49,50]. Additionally, in the “TCGA TARGET GTEx” dataset, the low-expression group also had lower survival than the high-expression group. Margin status and the presence of distant metastases could also be confounding variables in this dataset, but data were not available to determine that. In this way, we show that the relationship between LAT1 expression and survival in breast cancer patients may be more complicated than previously appreciated.

Past analyses on LAT1 are not stratified by menopausal status, another unique quality of our study. In breast cancer patients with high tumor LAT1 expression, we observed worse survival in postmenopausal individuals as compared to peri- or premenopausal, but interestingly, these relationships were not observed in patients with low LAT1 expression. This discrepancy may reflect the fact that LAT1 has been shown to be estrogen-dependent in endocrine-responsive cells [51,52]. Therefore, it is likely that more of the tumors in the low LAT1 group were triple-negative breast cancers, which generally have a poor prognosis independently of menopausal status. We recognize that worse survival is expected over the more than 10-year duration of follow-up in the datasets analyzed in postmenopausal patients, who are older and at greater risk for numerous conditions than their younger counterparts. Thus, the fact that survival differences were not observed in the LAT1 group implies that a regulator of LAT1 expression - such as estrogen - may obscure expected differences in survival. Additionally, we observed a positive correlation ($r < 0.5$) between BMI and basophil, eosinophil, monocyte, and lymphocyte counts in postmenopausal patients, a finding not seen in premenopausal patients. On the contrary, the opposite was observed in premenopausal patients. Premenopausal patients experience heightened 17β-estradiol levels, dampening obesity-induced inflammation, whereas postmenopausal patients (and those with obesity) have higher levels of estrone, stimulating inflammation. The imbalance between estrone and 17β-estradiol levels that occurs after menopause results in the release of cytokines and the recruitment of nearby immune cells, which likely explains this correlation only being observed in postmenopausal patients [53][s1].

^{18}F-fluorodeoxyglucose (^{18}F-FDG) has been the traditional radiotracer utilized in cancer research, and it is still used in the majority of tumor radiotracer analyses. Indeed, the Positron Emission Tomography Response Criteria in Solid Tumors (PERCIST) is based on the use of ^{18}F-FDG as the radiotracer [54,55]. However, although high ^{18}F-FDG uptake correlates with poor prognosis in numerous tumor types, including breast cancer [56–61], it is not a direct readout of tumor proliferative activity. For this, it is necessary to utilize a tracer such as ^{18}F-FLT, an analog of thymidine which is phosphorylated by thymidine kinase prior to incorporation into DNA during cell replication. Because our study employs ^{18}F-FLT imaging as a more direct readout of tumor proliferation rather than ^{18}F-FDG, we provide an analysis that has previously been insufficiently explored. We observe differences in the strength of the correlation between Ki-67 and ^{18}F-FLT uptake in pre- and postmenopausal patients: in postmenopausal patients, Ki-67 significantly positively correlated with ^{18}F-FLT SUV_{Mean}, SUV_{Peak}, and SUV_{Max}, whereas in premenopausal patients, Ki-67 insignificantly positively correlated with ^{18}F-FLT. These data are consistent with prior studies in which the correlation between Ki-67 and ^{18}F-FLT was found to be relatively weak and dependent on clinical variables (pre- or post-treatment timing, hormone receptor status) [62,63]. Surprisingly, BMI barely correlated with either Ki-67 or ^{18}F-FLT, which may mean that obesity is more involved in the appearance - and potentially recurrence - of cancer rather than its progression once a tumor is already established. Further work will be

required to better understand the nuanced relationships between these clinical variables. Additionally, it will be important to understand the relationship between LAT1 expression, ^{18}F-FLT uptake, and clinical variables including BMI and - better yet [64] - adiposity. In fact, to our knowledge, there are no studies correlating LAT1 expression to all 3 types of ^{18}F-FLT SUVs. We recognize that a limitation of our study is that BMI is not the best metric for obesity. In the datasets analyzed, there were no clinical data including possible alternatives for BMI like visceral adiposity, so we did not have an alternative to relying on BMI. Correlating ^{18}F-FLT uptake to both gene expression and a broad range of anthropometric indices, including visceral adiposity, will be of great interest in future studies.

Conclusion

Through our analyses, we show that although the extent to which this occurs is stratified by menopausal status, LAT1 expression worsens breast cancer prognosis, bolstering the role of amino acid metabolism in tumor energetics, an aspect of the literature that has been underexplored. Using various clinical variables, we correlated tumor proliferation, body composition, and immune cell populations to identify the complex relationships underlying metabolism, immune surveillance, and cancer progression. Future studies should aim to utilize a wider variety of immune cell types and metrics for body composition, while further segmenting patients based on breast cancer subtype, to gain a more comprehensive understanding of the findings we establish here. In addition, we speculate that future studies should target LAT1 or its heavy chain partner 4F2hc to inhibit the LAT1-4F2hc complex, interventions which may plausibly improve patient outcomes.

Acknowledgments

The authors are grateful for awards from the Lion Heart Foundation and from the Yale Cancer Center, which supported this research.

References

1. Tangka F, Yabroff R, Jingxuan Z, Mariotto A. The Cost of Cancer | Blogs | CDC. 26 Oct 2021 [cited 5 Jul 2023]. Available: https://blogs.cdc.gov/cancer/2021/10/26/the-cost-of-cancer/

2. Giaquinto AN, Sung H, Miller KD, Kramer JL, Newman LA, Minihan A, et al. Breast Cancer Statistics, 2022. CA: A Cancer Journal for Clinicians. 2022;72: 524–541. doi:10.3322/caac.21754

3. Liberti MV, Locasale JW. The Warburg Effect: How Does it Benefit Cancer Cells? Trends Biochem Sci. 2016;41: 211–218. doi:10.1016/j.tibs.2015.12.001

4. Wang D, Wan X. Progress in research on the role of amino acid metabolic reprogramming in tumour therapy: A review. Biomedicine & Pharmacotherapy. 2022;156: 113923. doi:10.1016/j.biopha.2022.113923

5. Yang L, Chu Z, Liu M, Zou Q, Li J, Liu Q, et al. Amino acid metabolism in immune cells: essential regulators of the effector functions, and promising opportunities to enhance cancer immunotherapy. J Hematol Oncol. 2023;16: 59. doi:10.1186/s13045-023-01453-1

6. Zhao Y, Wang L, Pan J. The role of L-type amino acid transporter 1 in human tumors. Intractable Rare Dis Res. 2015;4: 165–169. doi:10.5582/irdr.2015.01024

7. El Ansari R, Craze ML, Miligy I, Diez-Rodriguez M, Nolan CC, Ellis IO, et al. The amino acid transporter SLC7A5 confers a poor prognosis in the highly proliferative breast cancer subtypes and is a key therapeutic target in luminal B tumours. Breast Cancer Research. 2018;20: 21. doi:10.1186/s13058-018-0946-6

8. Yan R, Li Y, Müller J, Zhang Y, Singer S, Xia L, et al. Mechanism of substrate transport and inhibition of the human LAT1-4F2hc amino acid transporter. Cell Discov. 2021;7: 1–8. doi:10.1038/s41421-021-00247-4

9. Sanghera B, Wong WL, Sonoda LI, Beynon G, Makris A, Woolf D, et al. FLT PET-CT in evaluation of treatment response. Indian J Nucl Med. 2014;29: 65–73. doi:10.4103/0972-3919.130274

10. Kostakoglu L, Duan F, Idowu MO, Jolles PR, Bear HD, Muzi M, et al. A Phase II Study of 3′-Deoxy-3′-18F-Fluorothymidine PET in the Assessment of Early Response of Breast Cancer to Neoadjuvant Chemotherapy: Results from ACRIN 6688. J Nucl Med. 2015;56: 1681–1689. doi:10.2967/jnumed.115.160663

11. Chang ZF, Huang DY, Hsue NC. Differential phosphorylation of human thymidine kinase in proliferating and M phase-arrested human cells. Journal of Biological Chemistry. 1994;269: 21249–21254. doi:10.1016/S0021-9258(17)31956-7

12. PECK M, POLLACK HA, FRIESEN A, MUZI M, SHONER SC, SHANKLAND EG, et al. Applications of PET imaging with the proliferation marker [18F]-FLT. Q J Nucl Med Mol Imaging. 2015;59: 95–104.

13. Gerdes J, Schwab U, Lemke H, Stein H. Production of a mouse monoclonal antibody reactive with a human nuclear antigen associated with cell proliferation. Int J Cancer. 1983;31: 13–20. doi:10.1002/ijc.2910310104

14. García-Estévez L, Cortés J, Pérez S, Calvo I, Gallegos I, Moreno-Bueno G. Obesity and Breast Cancer: A Paradoxical and Controversial Relationship Influenced by Menopausal Status. Frontiers in Oncology. 2021;11. Available: https://www.frontiersin.org/articles/10.3389/fonc.2021.705911

15. Kinahan P, Muzi M, Bialecki B, Coombs L. Data from ACRIN-FLT-Breast. The Cancer Imaging Archive; 2017. doi:10.7937/K9/TCIA.2017.OL20ZMXG

16. Clark K, Vendt B, Smith K, Freymann J, Kirby J, Koppel P, et al. The Cancer Imaging Archive (TCIA): Maintaining and Operating a Public Information Repository. J Digit Imaging. 2013;26: 1045–1057. doi:10.1007/s10278-013-9622-7

17. Goldman MJ, Craft B, Hastie M, Repečka K, McDade F, Kamath A, et al. Visualizing and interpreting cancer genomics data via the Xena platform. Nat Biotechnol. 2020;38: 675–678. doi:10.1038/s41587-020-0546-8

18. Liu R, Ospanova S, Perry RJ. The impact of variance in carnitine palmitoyltransferase-1 expression on breast cancer prognosis is stratified by clinical and anthropometric factors. PLOS ONE. 2023;18: e0281252. doi:10.1371/journal.pone.0281252

19. Levine EG, Raczynski JM, Carpenter JT. Weight gain with breast cancer adjuvant treatment. Cancer. 1991;67: 1954–1959. doi:10.1002/1097-0142(19910401)67:7<1954::AID-CNCR2820670722>3.0.CO;2-Z

20. Uhelski A-CR, Blackford AL, Sheng JY, Snyder C, Lehman J, Visvanathan K, et al. Factors associated with weight gain in pre- and post-menopausal women receiving adjuvant endocrine therapy for breast cancer. J Cancer Surviv. 2023 [cited 5 Jul 2023]. doi:10.1007/s11764-023-01408-y

21. Walker J, Joy AA, Vos LJ, Stenson TH, Mackey JR, Jovel J, et al. Chemotherapy-induced weight gain in early-stage breast cancer: a prospective matched cohort study reveals associations with inflammation and gut dysbiosis. BMC Medicine. 2023;21: 178. doi:10.1186/s12916-023-02751-8

22. Ee C, Cave A, Vaddiparthi V, Naidoo D, Boyages J. Factors associated with weight gain after breast cancer: Results from a community-based survey of Australian women. The Breast. 2023;69: 491–498. doi:10.1016/j.breast.2023.01.012

23. Könik A, O'Donoghue JA, Wahl RL, Graham MM, Van den Abbeele AD. Theranostics: The Role of Quantitative Nuclear Medicine Imaging. Seminars in Radiation Oncology. 2021;31: 28–36. doi:10.1016/j.semradonc.2020.07.003

24. Grinde MT, Moestue SA, Borgan E, Risa Ø, Engebraaten O, Gribbestad IS. 13C High-resolution-magic angle spinning MRS reveals differences in glucose metabolism between two breast cancer xenograft models with different gene expression patterns. NMR in Biomedicine. 2011;24: 1243–1252. doi:10.1002/nbm.1683

25. Bawab AQA, Zihlif M, Jarrar Y, Sharab A. Continuous Hypoxia and Glucose Metabolism: The Effects on Gene Expression in Mcf7 Breast Cancer Cell Line. Endocrine, Metabolic & Immune Disorders - Drug Targets. 21: 511–519.

26. Cheng X, Jia X, Wang C, Zhou S, Chen J, Chen L, et al. Hyperglycemia induces PFKFB3 overexpression and promotes malignant phenotype of breast cancer through RAS/MAPK activation. World Journal of Surgical Oncology. 2023;21: 112. doi:10.1186/s12957-023-02990-2

27. Jekabsons MB, Merrell M, Skubiz AG, Thornton N, Milasta S, Green D, et al. Breast cancer cells that preferentially metastasize to lung or bone are more glycolytic, synthesize serine at greater rates, and consume less ATP and NADPH than parent MDA-MB-231 cells. Cancer & Metabolism. 2023;11: 4. doi:10.1186/s40170-023-00303-5

28. Tucker JD, Doddapaneni R, Lu PJ, Lu QL. Ribitol alters multiple metabolic pathways of central carbon metabolism with enhanced glycolysis: A metabolomics and transcriptomics profiling of breast cancer. PLOS ONE. 2022;17: e0278711. doi:10.1371/journal.pone.0278711

29. Zhu P, Liu G, Wang X, Lu J, Zhou Y, Chen S, et al. Transcription factor c-Jun modulates GLUT1 in glycolysis and breast cancer metastasis. BMC Cancer. 2022;22: 1283. doi:10.1186/s12885-022-10393-x

30. Ambrosio MR, Mosca G, Migliaccio T, Liguoro D, Nele G, Schonauer F, et al. Glucose Enhances Pro-Tumorigenic Functions of Mammary Adipose-Derived Mesenchymal Stromal/Stem Cells on Breast Cancer Cell Lines. Cancers (Basel). 2022;14: 5421. doi:10.3390/cancers14215421

31. Lee R, Lee H-B, Paeng JC, Choi H, Whi W, Han W, et al. Association of androgen receptor expression with glucose metabolic features in triple-negative breast cancer. PLOS ONE. 2022;17: e0275279. doi:10.1371/journal.pone.0275279

32. Monaco ME. ACSL4: biomarker, mediator and target in quadruple negative breast cancer. Oncotarget. 2023;14: 563–575. doi:10.18632/oncotarget.28453

33. Tang L, Lei X, Hu H, Li Z, Zhu H, Zhan W, et al. Investigation of fatty acid metabolism-related genes in breast cancer: Implications for Immunotherapy and clinical significance. Translational Oncology. 2023;34: 101700. doi:10.1016/j.tranon.2023.101700

34. Miyashita M, Bell JSK, Wenric S, Karaesmen E, Rhead B, Kase M, et al. Molecular profiling of a real-world breast cancer cohort with genetically inferred ancestries reveals actionable tumor biology differences between European ancestry and African ancestry patient populations. Breast Cancer Research. 2023;25: 58. doi:10.1186/s13058-023-01627-2

35. Qian L, Liu Y-F, Lu S-M, Yang J-J, Miao H-J, He X, et al. Construction of a fatty acid metabolism-related gene signature for predicting prognosis and immune response in breast cancer. Front Genet. 2023;14: 1002157. doi:10.3389/fgene.2023.1002157

36. Qian Z, Chen L, Liu J, Jiang Y, Zhang Y. The emerging role of PPAR-alpha in breast cancer. Biomedicine & Pharmacotherapy. 2023;161: 114420. doi:10.1016/j.biopha.2023.114420

37. Yousuf U, Sofi S, Makhdoomi A, Mir MA. Identification and analysis of dysregulated fatty acid metabolism genes in breast cancer subtypes. Med Oncol. 2022;39: 256. doi:10.1007/s12032-022-01861-2

38. Chang X, Xing P. Identification of a novel lipid metabolism-related gene signature within the tumour immune microenvironment for breast cancer. Lipids in Health and Disease. 2022;21: 43. doi:10.1186/s12944-022-01651-9

39. Pham D-V, Park P-H. Adiponectin triggers breast cancer cell death via fatty acid metabolic reprogramming. Journal of Experimental & Clinical Cancer Research. 2022;41: 9. doi:10.1186/s13046-021-02223-y

40. Collao N, Akohene-Mensah P, Nallabelli J, Binet ER, Askarian A, Lloyd J, et al. The role of L-type amino acid transporter 1 (Slc7a5) during in vitro myogenesis. American Journal of Physiology-Cell Physiology. 2022;323: C595–C605. doi:10.1152/ajpcell.00162.2021

41. Nishikubo K, Ohgaki R, Okanishi H, Okuda S, Xu M, Endou H, et al. Pharmacologic inhibition of LAT1 predominantly suppresses transport of large neutral amino acids and downregulates global translation in cancer cells. Journal of Cellular and Molecular Medicine. 2022;26: 5246–5256. doi:10.1111/jcmm.17553

42. Chiduza GN, Johnson RM, Wright GSA, Antonyuk SV, Muench SP, Hasnain SS. LAT1 (SLC7A5) and CD98hc (SLC3A2) complex dynamics revealed by single-particle cryo-EM. Acta Crystallogr D Struct Biol. 2019;75: 660–669. doi:10.1107/S2059798319009094

43. Li Y, Wang W, Wu X, Ling S, Ma Y, Huang P. SLC7A5 serves as a prognostic factor of breast cancer and promotes cell proliferation through activating AKT/mTORC1 signaling pathway. Ann Transl Med. 2021;9: 892. doi:10.21037/atm-21-2247

44. Solvay M, Holfelder P, Klaessens S, Pilotte L, Stroobant V, Lamy J, et al. Tryptophan depletion sensitizes the AHR pathway by increasing AHR expression and GCN2/LAT1-mediated kynurenine uptake, and potentiates induction of regulatory T lymphocytes. J Immunother Cancer. 2023;11: e006728. doi:10.1136/jitc-2023-006728

608 45. Tian X, Liu X, Ding J, Wang F, Wang K, Liu J, et al. An anti-CD98 antibody displaying pH-
609 dependent Fc-mediated tumour-specific activity against multiple cancers in CD98-
610 humanized mice. Nat Biomed Eng. 2023;7: 8–23. doi:10.1038/s41551-022-00956-5

611 46. Liu Y-H, Li Y-L, Shen H-T, Chien P-J, Sheu G-T, Wang B-Y, et al. L-Type Amino Acid
612 Transporter 1 Regulates Cancer Stemness and the Expression of Programmed Cell Death 1
613 Ligand 1 in Lung Cancer Cells. Int J Mol Sci. 2021;22: 10955. doi:10.3390/ijms222010955

614 47. Kuriyama K, Higuchi T, Yokobori T, Saito H, Yoshida T, Hara K, et al. Uptake of positron
615 emission tomography tracers reflects the tumor immune status in esophageal squamous cell
616 carcinoma. Cancer Sci. 2020;111: 1969–1978. doi:10.1111/cas.14421

617 48. Häfliger P, Charles R-P. The L-Type Amino Acid Transporter LAT1—An Emerging Target
618 in Cancer. Int J Mol Sci. 2019;20: 2428. doi:10.3390/ijms20102428

619 49. Xiao W, Zheng S, Yang A, Zhang X, Zou Y, Tang H, et al. Breast cancer subtypes and the
620 risk of distant metastasis at initial diagnosis: a population-based study. Cancer Manag Res.
621 2018;10: 5329–5338. doi:10.2147/CMAR.S176763

622 50. Bundred JR, Michael S, Stuart B, Cutress RI, Beckmann K, Holleczek B, et al. Margin status
623 and survival outcomes after breast cancer conservation surgery: prospectively registered
624 systematic review and meta-analysis. BMJ. 2022;378: e070346. doi:10.1136/bmj-2022-
625 070346

626 51. Sevigny CM, Sengupta S, Luo Z, Liu X, Hu R, Zhang Z, et al. SLCs contribute to endocrine
627 resistance in breast cancer: role of SLC7A5 (LAT1). bioRxiv; 2019. p. 555342.
628 doi:10.1101/555342

629 52. Shennan DB, Thomson J, Gow IF, Travers MT, Barber MC. l-Leucine transport in human
630 breast cancer cells (MCF-7 and MDA-MB-231): kinetics, regulation by estrogen and
631 molecular identity of the transporter. Biochimica et Biophysica Acta (BBA) -
632 Biomembranes. 2004;1664: 206–216. doi:10.1016/j.bbamem.2004.05.008

633 53. Qureshi R, Picon-Ruiz M, Aurrekoetxea-Rodriguez I, Paiva VN de, D'Amico M, Yoon H, et
634 al. The Major Pre- and Postmenopausal Estrogens Play Opposing Roles in Obesity-Driven
635 Mammary Inflammation and Breast Cancer Development. Cell Metabolism. 2020;31: 1154-
636 1172.e9. doi:10.1016/j.cmet.2020.05.008

637 54. Sato M, Harada-Shoji N, Toyohara T, Soga T, Itoh M, Miyashita M, et al. L-type amino acid
638 transporter 1 is associated with chemoresistance in breast cancer via the promotion of amino
639 acid metabolism. Sci Rep. 2021;11: 589. doi:10.1038/s41598-020-80668-5

640 55. Kitajima K, Nakatani K, Yamaguchi K, Nakajo M, Tani A, Ishibashi M, et al. Response to
641 neoadjuvant chemotherapy for breast cancer judged by PERCIST - multicenter study in
642 Japan. Eur J Nucl Med Mol Imaging. 2018;45: 1661–1671. doi:10.1007/s00259-018-4008-1

643 56. Cremoux P de, Biard L, Poirot B, Bertheau P, Teixeira L, Lehmann-Che J, et al. 18 FDG-
644 PET/CT and molecular markers to predict response to neoadjuvant chemotherapy and

outcome in HER2-negative advanced luminal breast cancers patients. Oncotarget. 2018;9: 16343–16353. doi:10.18632/oncotarget.24674

57. Groheux D, Martineau A, Teixeira L, Espié M, de Cremoux P, Bertheau P, et al. 18FDG-PET/CT for predicting the outcome in ER+/HER2- breast cancer patients: comparison of clinicopathological parameters and PET image-derived indices including tumor texture analysis. Breast Cancer Research. 2017;19: 3. doi:10.1186/s13058-016-0793-2

58. Humbert O, Riedinger J-M, Charon-Barra C, Berriolo-Riedinger A, Desmoulins I, Lorgis V, et al. Identification of Biomarkers Including 18FDG-PET/CT for Early Prediction of Response to Neoadjuvant Chemotherapy in Triple-Negative Breast Cancer. Clin Cancer Res. 2015;21: 5460–5468. doi:10.1158/1078-0432.CCR-15-0384

59. Groheux D, Sanna A, Majdoub M, Cremoux P de, Giacchetti S, Teixeira L, et al. Baseline Tumor 18F-FDG Uptake and Modifications After 2 Cycles of Neoadjuvant Chemotherapy Are Prognostic of Outcome in ER+/HER2− Breast Cancer. Journal of Nuclear Medicine. 2015;56: 824–831. doi:10.2967/jnumed.115.154138

60. Cochet A, David S, Moodie K, Drummond E, Dutu G, MacManus M, et al. The utility of 18 F-FDG PET/CT for suspected recurrent breast cancer: impact and prognostic stratification. Cancer Imaging. 2014;14: 13. doi:10.1186/1470-7330-14-13

61. Jacobs MA, Ouwerkerk R, Wolff AC, Gabrielson E, Warzecha H, Jeter S, et al. Monitoring of neoadjuvant chemotherapy using multiparametric, ^{23}Na sodium MR, and multimodality (PET/CT/MRI) imaging in locally advanced breast cancer. Breast Cancer Res Treat. 2011;128: 119–126. doi:10.1007/s10549-011-1442-1

62. Romine PE, Peterson LM, Kurland BF, Byrd DW, Novakova-Jiresova A, Muzi M, et al. 18F-fluorodeoxyglucose (FDG) PET or 18F-fluorothymidine (FLT) PET to assess early response to aromatase inhibitors (AI) in women with ER+ operable breast cancer in a window-of-opportunity study. Breast Cancer Research. 2021;23: 88. doi:10.1186/s13058-021-01464-1

63. Su T-P, Huang J-S, Chang P-H, Lui K-W, Hsieh JC-H, Ng S-H, et al. Prospective comparison of early interim 18F-FDG-PET with 18F-FLT-PET for predicting treatment response and survival in metastatic breast cancer. BMC Cancer. 2021;21: 908. doi:10.1186/s12885-021-08649-z

64. Leitner BP, Givechian KB, Ospanova S, Beisenbayeva A, Politi K, Perry RJ. Multimodal analysis suggests differential immuno-metabolic crosstalk in lung squamous cell carcinoma and adenocarcinoma. npj Precis Onc. 2022;6: 1–10. doi:10.1038/s41698-021-00248-2